

**Decay of zone-center phonons in AlN with  $A_1$ ,  $E_1$ , and  $E_2$  symmetries**P. Pandit, D. Y. Song, and M. Holtz<sup>a)</sup>*Texas Tech University, Lubbock, Texas 79409, USA*

(Received 3 September 2007; accepted 12 October 2007; published online 6 December 2007)

Raman studies are reported for the  $A_1(\text{TO})$ ,  $E_1(\text{TO})$ ,  $E_2^2$ , and  $A_1(\text{LO})$  symmetry phonons of AlN from 20 to 375 K. By applying anharmonic decay theory to the observed temperature dependences of the phonon energies and linewidths, we determine the phonon decay mechanisms of these zone-center vibrations. Thermal expansion is taken into account using published temperature-dependent coefficients. The  $A_1(\text{TO})$ ,  $E_1(\text{TO})$ , and  $E_2^2$  vibrations are described by symmetric two-phonon decay. The  $A_1(\text{LO})$  band is interpreted by an asymmetric two-phonon decay. Phonon lifetimes are obtained based on the observed linewidths and the dependence allows us to estimate the impurity-related phonon lifetime for each vibration. The latter ranges from 2.9 to 9.1 ps. © 2007 American Institute of Physics. [DOI: 10.1063/1.2821360]

**I. INTRODUCTION**

Persistent efforts at miniaturizing optoelectronic and electronic devices produce situations with high current density, such as crowding in bipolar transistors and quasi-two-dimensional electron gases in field effect transistors. This results in significant local self-heating<sup>1,2</sup> which degrades performance and is an important failure mechanism. In polar materials, such as the III-nitrides, dissipation of hot electron energy is predominantly through Fröhlich electron-phonon scattering. Due to the form of the Fröhlich interaction, this carrier relaxation process primarily produces zone-center longitudinal-optic (LO) phonons.<sup>3</sup> The zone-center LO phonons behave like standing waves and must decay into traveling acoustic waves to dissipate energy from the immediate self-heating region. Understanding the intrinsic phonon decay properties of high-quality crystalline materials is thus fundamental to self-heating and phonon engineering aimed at mitigating the associated device problems.

The  $\mathbf{q}=0$  selection rule of Raman scattering in crystals, where  $\mathbf{q}$  is the wave vector, makes this measurement ideal for studying the zone-center phonons which are produced by carrier relaxation in polar semiconductors. Phonon lifetimes are often studied through measured Raman linewidths ( $\Gamma$ ), which are inversely proportional to the overall phonon lifetime ( $\tau_{\text{total}}$ ). The phonon lifetime is generally influenced by anharmonic decay and inhomogeneous impurity phonon scattering according to

$$2\pi c\Gamma = \frac{1}{\tau_{\text{total}}} = \frac{1}{\tau_{\text{decay}}} + \frac{1}{\tau_i}, \quad (1)$$

where  $c$  is the speed of light in cm/s and  $\Gamma$  is in  $\text{cm}^{-1}$ . The average phonon decay time is  $\tau_{\text{decay}}$ , while  $\tau_i$  represents the net effect of impurity and defect phonon scattering processes. For high-quality crystalline materials,  $1/\tau_i$  is generally taken as small and temperature independent. When impurity scattering is negligible in comparison to the

anharmonic processes, direct measurement of  $\Gamma$  can be used to estimate the decay time  $\tau_{\text{decay}}$ .

Phonons may decay into two or more lower energy vibrations providing total energy and wave vector are each conserved. Decay processes producing vibrations with high phonon joint density of states dominate and lower order processes generally have higher probability when they satisfy the above stipulations. The prevailing two-phonon decay mechanisms are referred to as Klemens<sup>4</sup> and Ridley processes.<sup>5</sup> In the Klemens process, an optical phonon decays symmetrically into two identical acoustic phonons with opposite momenta. The Ridley process corresponds to the asymmetric decay of one LO phonon into one transverse optical (TO) phonon and one longitudinal acoustic (LA) phonon. The Ridley channel is relevant when large energy differences exist between optic and acoustic branches caused by the large differences in anion and cation masses. When the two-phonon process does not fully describe the phonon decay mechanism, it is usual to include third—or higher-order phonon decay processes.

Temperature dependent Raman scattering studies are useful for examining zone-center phonon decay processes in high-quality crystals. The phonon energy and linewidth may both be accurately described according to the phonon decay model. Previous reports concerning phonon decay have used Raman scattering to examine the  $E_2^2$  and  $A_1(\text{LO})$  phonon decay properties in AlN (Refs. 6 and 7) since these phonons are allowed in the (0001) backscattering configuration and therefore readily measurable. For the III-nitride materials the decay properties of zone-center phonons, other than  $A_1(\text{LO})$  and  $E_2^2$ , have been reported for GaN.<sup>8,9</sup> In this paper, we study the  $A_1(\text{TO})$ ,  $E_1(\text{TO})$ ,  $E_2^2$ , and  $A_1(\text{LO})$  phonons in bulk AlN and examine their decay properties based on anharmonic theory.

**II. PHONON DECAY**

An overview of phonon decay theory has been recently published focusing on sibling material GaN.<sup>9</sup> The temperature ( $T$ ) dependence is described by the phonon population at thermal equilibrium according to the Bose function  $n_j(\mathbf{q}, T)$

<sup>a)</sup>Author to whom correspondence should be addressed. Electronic mail: mark.holtz@ttu.edu

$=\{\exp[hc\omega_j(\mathbf{q})/k_B T]-1\}^{-1}$  at energy  $hc\omega_j$ . Subscript  $j$  denotes the phonon branch and  $\omega_j$  is in  $\text{cm}^{-1}$ . Within the single-mode relaxation time approach,<sup>10</sup> the initial phonon at  $\mathbf{q}=0$  has a nonequilibrium population and phonons at all other points of the Brillouin zone are assumed to be in equilibrium. In our experiments, the nonequilibrium abundance of  $\mathbf{q}=0$  phonons arises from the Raman process. In situations where phonon decay processes may be attributed to a single (or narrow) set of created phonons, the temperature dependence of the phonon energy  $\omega(T)$  can be approximated according to the lowest order anharmonic (thermal expansion) contribution<sup>11</sup>

$$\omega(T) = \omega_0 + \Delta_0(T) + A(1 + n_1 + n_2), \quad (2)$$

where  $\omega_0$  is the harmonic frequency of the phonon mode and  $\Delta_0(T)$  is the thermal expansion contribution to the frequency. Explicit wave vector and temperature dependences of the Bose functions have been suppressed. We account here for two-phonon decay only. When three or more vibrations are produced, then additional terms are included to describe the temperature dependence. Coefficient  $A$  depends on the specific decay and is a measure of its importance when competing processes take place. The thermal expansion contribution is given by  $\Delta_0(T) = -\omega_0 \gamma \int_0^T [\alpha_c(T') + 2\alpha_a(T')] dT'$ , where  $\gamma$  is the Gruneisen parameter and  $\alpha_c$  and  $\alpha_a$  are the linear thermal expansion coefficients along and transverse to the hexagonal  $c$  axis, respectively. Recent work points out the importance of using the temperature dependent thermal expansion coefficients when examining the decay processes in GaN (Refs. 9 and 12) and AlN.<sup>7</sup> Based on published values for  $\alpha_c$  and  $\alpha_a$ ,<sup>13</sup> and for  $\gamma$ ,<sup>14</sup>  $\Delta_0(T)$  may be calculated without any fitting parameters.

The temperature dependence of  $\Gamma(T)$  has a form analogous to Eq. (2),

$$\Gamma(T) = \Gamma_0 + 2C(1 + n_1 + n_2), \quad (3)$$

where  $\Gamma_0 + 2C$  is the  $T \rightarrow 0$  phonon linewidth. In this paper, we use Eqs. (2) and (3) to fit the temperature dependences of measured Raman bands. By fitting both phonon energy and linewidth dependences, we obtain a detailed description of the decay processes involved for each AlN phonon studied. Because the energy shifts and linewidths are related by a Kramers-Kronig transformation, the coefficients  $A$  and  $C$  in Eqs. (2) and (3) should be in agreement provided a single mechanism is dominant and the matrix elements describing the process are independent of energy.<sup>9</sup> Examining Eqs. (1) and (3), we see that the results from fitting Eq. (3) to measured  $T$  dependences of  $\Gamma$  may also be used to obtain information about the impurity-related phonon lifetime  $\tau_i$ , since the second term in Eq. (3) may be attributed to the phonon decay rate  $1/\tau_{\text{decay}}$ , taking into account the factor  $2\pi c$ .

### III. EXPERIMENTAL DETAILS

AlN ingots were grown by sublimation sandwich technique described elsewhere.<sup>15</sup> X-ray diffraction reveals the AlN to be strain relaxed, with  $\omega$ -scan linewidths of 25 and 38 arc sec for (0002) and (11 $\bar{2}$ 4) reflections, respectively.<sup>7</sup> Micro-Raman measurements were made using 488.0 nm ex-

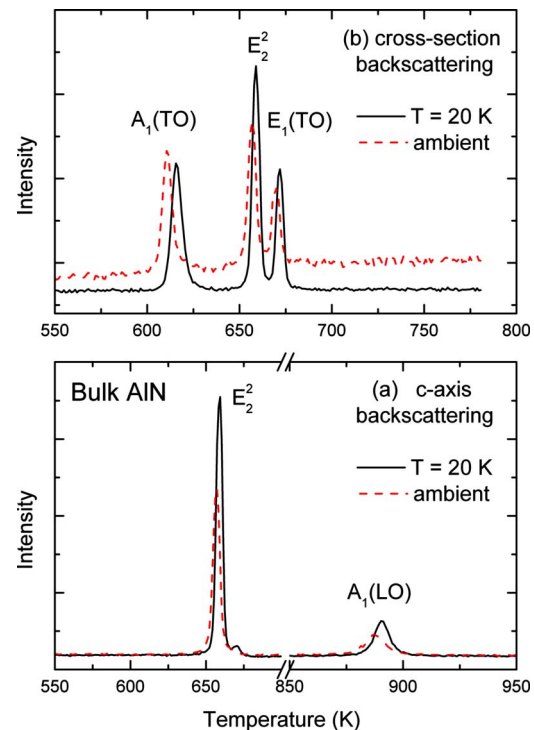


FIG. 1. (Color online) Raman spectra of AlN observed for different scattering geometries at  $T=20$  and 300 K. Backscattering along the (0001) crystal growth axis (a). Backscattering from the cross section (b).

citation and with the sample temperature controlled using a closed-cycle cryostat. Measurements were carried out from the polished (0001) surface of the sample and with it oriented edge on. This material exhibits narrow Raman bands allowing investigation of the linewidth and its implications in phonon lifetime. Spectra were fitted using a Lorentzian line shape. The reported linewidths are corrected for the  $2.4 \text{ cm}^{-1}$  instrumental bandpass of the Raman system. Representative spectra at low and ambient temperatures are shown in Fig. 1. The backscattering configuration was used for these measurements.<sup>16</sup> For the (0001) surface, we use the  $z(y,u)\bar{z}$  geometry in the standard Porto notation, while the cross-section measurements were carried out in the  $x(y,u)\bar{x}$  configuration. Here, the  $z$  or  $c$  axis is the (0001) crystal direction and  $x$  and  $y$  are perpendicular to  $z$  and correspond to conventional  $a$  and  $b$  directions. Symbol  $u$  indicates that polarization is not analyzed.

### IV. RESULTS

The phonon energies and linewidths of the  $A_1(\text{TO})$  and  $E_1(\text{TO})$  symmetry phonons are shown as functions of temperature in Figs. 2 and 3, respectively. Phonon lifetime values obtained using Eq. (1) are also shown (right-hand axes of respective linewidth graphs). The  $A_1(\text{TO})$  and  $E_1(\text{TO})$  exhibit similar dependences, although the shift is greater for the  $A_1(\text{TO})$  over the full temperature range examined. In each case, we fit the energy shift dependence using Eq. (2) and the line broadening using Eq. (3). Fit results are summarized in Table I.

For the  $A_1(\text{TO})$  phonon we find two-phonon decay adequately describes the data with  $\omega_1 = \omega_2 \sim 308 \text{ cm}^{-1}$ , corre-

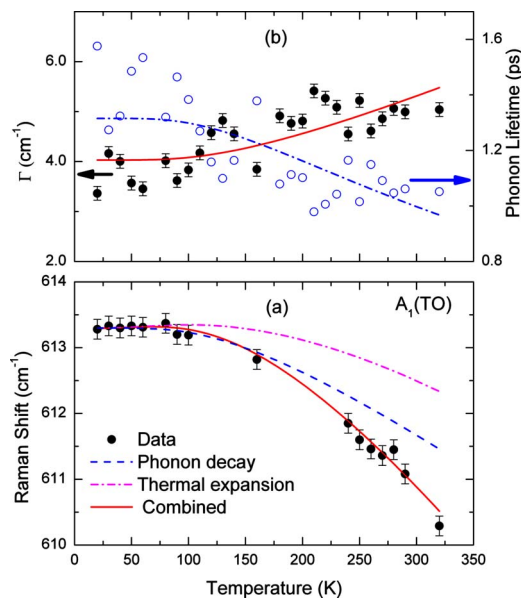


FIG. 2. (Color online) Dependence of  $A_1(\text{TO})$  phonon energies (a) and linewidths (b) on temperature. Curves are theory-based fits to data. Contributions of thermal expansion and phonon decay to the overall shifts are plotted separately. Phonon lifetime as a function of temperature is also shown in (b).

sponding to the symmetric Klemens channel. In Fig. 2(a), we also show the individual contributions of thermal expansion and phonon decay to the temperature shift. Thermal expansion accounts for only a small part of the observed shift across the full temperature range, while the majority of the shift is attributed to the phonon decay. Temperature-induced broadening is weak for this phonon,  $\sim 1 \text{ cm}^{-1}$  from 20 to 325 K. We analyze the temperature dependence of the  $A_1(\text{TO})$  broadening using the same values for  $\omega_1$  and  $\omega_2$  obtained from the phonon shift and fit Eq. (3) to linewidth data varying parameters  $\Gamma_0$  and  $C$ , as shown by the solid

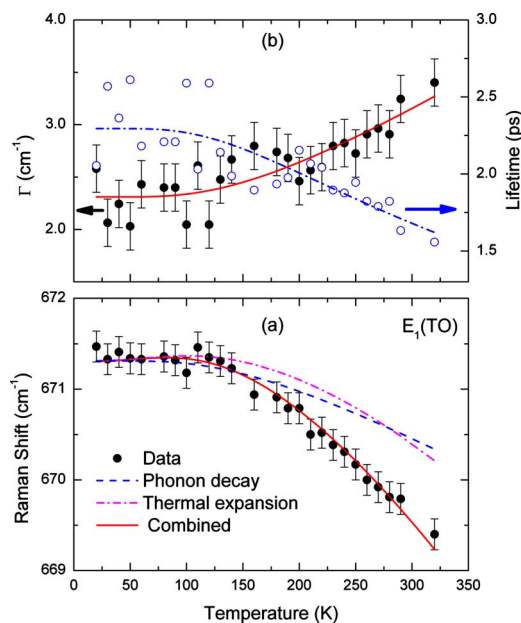


FIG. 3. (Color online) Dependence of  $E_1(\text{TO})$  phonon energies (a) and linewidths (b) on temperature, similar to Fig. 2.

TABLE I. Fitting results for Raman phonons of AlN. All  $T=0 \text{ K}$  values are from fits to the temperature dependences.

Symmetry	Energy	Linewidth
$A_1(\text{TO})$	$\omega_0=616.1 \pm 1.0 \text{ cm}^{-1}$ $A=2.76 \pm 1.03 \text{ cm}^{-1}$ $\omega_1=307.5 \text{ cm}^{-1}, \omega_2=309.6 \text{ cm}^{-1}$	$\Gamma_0=1.86 \pm 0.50 \text{ cm}^{-1}$ $C=1.09 \pm 0.20 \text{ cm}^{-1}$ $\tau_l=2.9 \pm 0.8 \text{ ps}$
$E_1(\text{TO})$	$\omega_0=673.0 \pm 0.1 \text{ cm}^{-1}$ $A=1.73 \pm 0.11 \text{ cm}^{-1}$ $\omega_1=\omega_2=336.5 \text{ cm}^{-1}$	$\Gamma_0=0.61 \pm 0.26 \text{ cm}^{-1}$ $C=0.85 \pm 0.11 \text{ cm}^{-1}$ $\tau_l=9.1 \pm 3.9 \text{ ps}$
$E_2^2$	$\omega_0=661.1 \pm 0.3 \text{ cm}^{-1}$ $A=2.37 \pm 0.37 \text{ cm}^{-1}$ $\omega_1=329.9 \text{ cm}^{-1}, \omega_2=331.2 \text{ cm}^{-1}$	$\Gamma_0=0.70 \pm 0.55 \text{ cm}^{-1}$ $C=1.06 \pm 0.29 \text{ cm}^{-1}$ $\tau_l=7.7 \pm 6.0 \text{ ps}$
$A_1(\text{LO})$	$\omega_0=895.1 \pm 0.3 \text{ cm}^{-1}$ $A=4.49 \pm 0.27 \text{ cm}^{-1}$ $\omega_1=586.1 \text{ cm}^{-1}, \omega_2=309 \text{ cm}^{-1}$	$\Gamma_0=0.93 \pm 0.38 \text{ cm}^{-1}$ $C=2.86 \pm 0.17 \text{ cm}^{-1}$ $\tau_l=5.9 \pm 2.4 \text{ ps}$

curve in Fig. 2(b). The fit agrees well with the experimental data consistently showing the decay of  $A_1(\text{TO})$  into two phonons with identical energies. The corresponding fit to the phonon lifetime is also shown in the upper panel. Examination of the AlN phonon dispersion<sup>17</sup> suggests that symmetric decay of the zone-center  $A_1(\text{TO})$  may be attributed to the production of two LA phonons near the  $M$  symmetry point of the Brillouin zone.

We similarly analyze the  $E_1(\text{TO})$  line, as shown in Fig. 3. The shift is described by approximately equal parts of the thermal expansion factor  $\Delta_0(T)$  and phonon decay. The linewidth broadens by  $\sim 1 \text{ cm}^{-1}$  over the temperature range studied, similar to what we see for the  $A_1(\text{TO})$ . The  $E_1(\text{TO})$  phonon symmetrically decays via creation of two phonons with energy of  $\sim 337 \text{ cm}^{-1}$ . Fitting results are consistent for both the Raman shifts and linewidths. Based on the phonon dispersion of AlN,<sup>17</sup> the  $E_1(\text{TO})$  decay produces LA phonons near the high density of states  $A$  and  $K$  points in the Brillouin zone. We notice the change of  $E_1(\text{TO})$  phonon linewidth remains smaller than the corresponding values of the  $A_1(\text{TO})$  band across the temperature range studied here. This indicates that the phonon decay process is weaker for the  $E_1(\text{TO})$  phonon, and we find a commensurately smaller coefficient  $A$ . A similar relationship was observed for the  $A_1(\text{TO})$  and  $E_1(\text{TO})$  phonons of GaN (Ref. 9) and attributed to a narrower range of phonons in the Brillouin zone participating in the  $E_1(\text{TO})$  decay process.

The  $E_2^2$  band exhibits a slightly stronger temperature dependence than the TO phonons, redshifting by  $\sim 5 \text{ cm}^{-1}$  and broadening  $\sim 2 \text{ cm}^{-1}$  across the temperature range studied (Fig. 4). The contribution to the overall shift from phonon decay is slightly larger than what is calculated based on thermal expansion  $\Delta_0(T)$ . Analysis of the temperature dependence shows that the decay of  $E_2^2$  is described by a two-phonon process producing acoustic phonons at  $\sim 330 \text{ cm}^{-1}$ . Regions of the Brillouin zone, which may contribute to this decay process, are near the  $M$  and  $L$  symmetry points. In contrast to AlN, the  $E_2^2$  phonon in GaN exhibits a very small dependence across the same temperature range. This is attributed to the absence of a two-phonon decay channel for

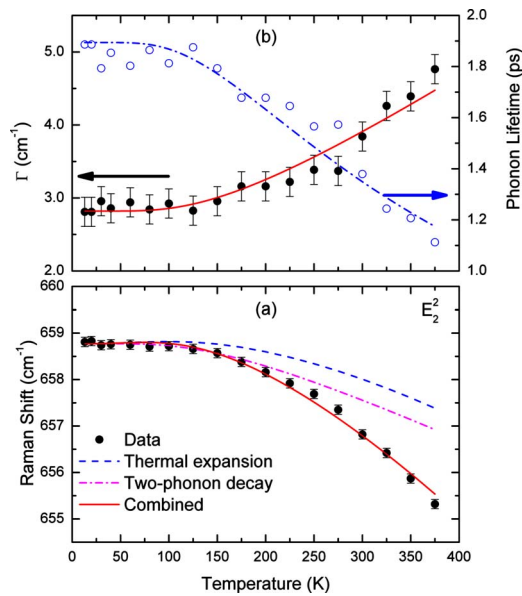


FIG. 4. (Color online) Dependence of  $E_2^2$  phonon energies (a) and linewidths (b) on temperature, similar to Fig. 2.

the  $E_2^2$  phonon of GaN and is illustrative of a case where three-phonon decay is dominant. The distinction is a result of the different phonon band structures of these two materials.

Turning our attention to the  $A_1(\text{LO})$  phonon, we analyze the temperature dependence shown in Fig. 5. Similar to the  $E_1(\text{TO})$  and  $E_2^2$  phonon dependences, the contribution from the two-phonon decay process is comparable in magnitude to that from thermal expansion. Our analysis suggests that the  $A_1(\text{LO})$  phonon exhibits asymmetric decay, i.e.,  $\omega_1 \neq \omega_2$ , producing one TO phonon with energy of 586 cm<sup>-1</sup> and one LA phonon with energy of 309 cm<sup>-1</sup>. Results are summarized in Table I. The  $A_1(\text{LO})$  phonon linewidth data are shown in Fig. 5(b). Again, we find good agreement with the data when parameters  $\omega_1$  and  $\omega_2$  are fixed at the values ob-

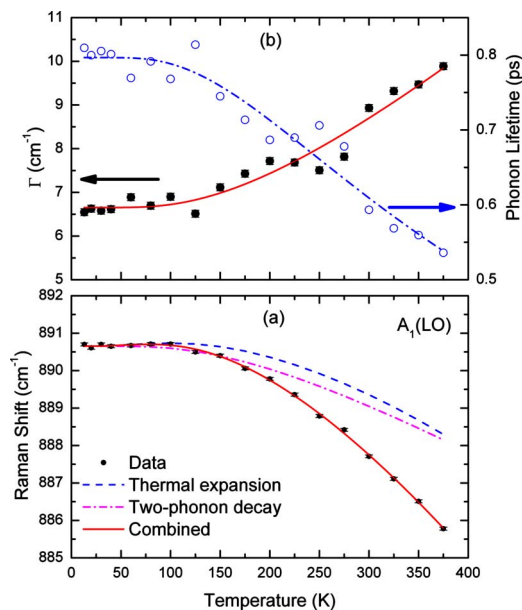


FIG. 5. (Color online) Dependence of  $A_1(\text{LO})$  phonon energies (a) and linewidths (b) on temperature, similar to Fig. 2.

tained from fitting the phonon energy dependence and parameters  $\Gamma_0$  and  $C$  are varied to fit the data. This consistency strongly supports the decay of  $A_1(\text{LO})$  phonon into one TO phonon and one LA phonon as the most possible decay channel, in agreement with Ref. 7. From published phonon dispersion curves for AlN,<sup>17</sup> the created phonons may be attributed to the  $A_1(\text{TO})$  and LA vibrations near the  $M$  point and possibly the  $B_1$  and  $E_2^1$  vibrations from the  $L$  point of the Brillouin zone. The former decay assignment is the Ridley channel.<sup>5</sup>

## V. DISCUSSION

As mentioned in Sec. II, coefficients  $A$  and  $C$  in Eqs. (2) and (3) should be in agreement provided a single decay mechanism is dominant and the matrix elements describing the process are independent of energy.<sup>9</sup> We see from Table I that these fitting coefficients agree with each other for each phonon within a factor of  $\sim 2$ . This overall agreement is more consistent than what was observed for GaN, where the TO phonons exhibited  $C$  values approximately five times the  $A$  coefficients.<sup>9</sup> This was attributed to competing channels and the possibility that the matrix elements which describe the phonon decay process are independent of energy. Coefficients  $A$  and  $C$  for the LO phonons of GaN, however, showed good agreement similar to what we report here for AlN. The assumption used here, that each AlN phonon decay studied may be attributed to a predominant channel, is supported by the consistency of the  $A$  and  $C$  parameters.

The low-temperature phonon lifetimes obtained for AlN from our studies are  $1.3 \pm 0.1$ ,  $2.3 \pm 0.2$ ,  $1.9 \pm 0.2$ , and  $0.8 \pm 0.2$  ps for  $A_1(\text{TO})$ ,  $E_1(\text{TO})$ ,  $E_2^2$ , and  $A_1(\text{LO})$ , respectively. These results compare well with previously published Raman work for the  $E_2^2$  and  $A_1(\text{LO})$  phonons with reported values of 3.0 and 0.75 ps, respectively.<sup>6</sup> Published phonon lifetimes based on low-temperature measurements of the  $A_1(\text{TO})$ ,  $E_1(\text{TO})$ ,  $E_2^2$ , and  $A_1(\text{LO})$  Raman bands are likewise consistent, with respective values of 0.76, 0.91, 0.83, and 0.45 ps.<sup>18</sup> Our AlN phonon lifetime values may also be compared with GaN, which range from 0.9 to 1.5 for the TO and LO phonons at low  $T$ .<sup>9</sup> The  $E_2^2$  vibration of GaN decays much slower, with lifetime of  $\sim 3.5$  ps at low  $T$  and exhibiting a very shallow temperature dependence. This behavior is attributed to the absence of a two-phonon decay mechanism for the  $E_2^2$  in GaN.<sup>9</sup> The Raman linewidth is commonly used as an indicator of crystal quality. The impurity-related decay rate  $1/\tau_i$  is a better indication of crystal quality than the total decay rate in Eq. (1). This is because the total decay rate is a convolution of impurity and phonon decay processes. The former are affected by impurities and defects, while the latter should be material independent for crystals having high quality. In Table I we include decay times  $\tau_i$  obtained from our analysis of the linewidth data. The values are consistent with each other, ranging from  $\sim 2.9$  to 9.1 ps. While we do not find any reports of direct phonon life time measurements in AlN, via time-resolved Raman scattering, GaN (Ref. 19) and InN (Ref. 20) have been examined. At low temperature, the published  $A_1(\text{LO})$  phonon lifetimes are 5.0 and 2.5 ps for

GaN and InN, respectively. These values are in reasonable agreement with what we report for  $\tau_i$  of the  $A_1(\text{LO})$  phonon in AlN.

## VI. SUMMARY

In agreement with previously published work,<sup>7,12</sup> we find the  $A_1(\text{LO})$  vibration primarily decays via Ridley two-phonon creation. The results suggest decay into vibrations with energies 586 and 309  $\text{cm}^{-1}$ . The  $A_1(\text{TO})$  and  $E_1(\text{TO})$  phonons both decay symmetrically into vibrations from the high density of states regions in the  $\sim 308$  and  $\sim 337$   $\text{cm}^{-1}$  range, respectively. The  $E_2^2$  phonon is also found to decay symmetrically into two phonons near 330  $\text{cm}^{-1}$ . This is also in agreement with prior publications.<sup>7</sup> The thermal expansion factor,  $\Delta_0(T)$ , has a significant effect on the temperature-induced redshift for each band. For each phonon studied here, the phonon shift and linewidth broadening fit parameters,  $A$  and  $C$ , consistently agree. Phonon lifetimes are all found to be in the 1–2 ps range and decrease with  $T$  due to rising phonon-assisted decay. The impurity-related phonon decay lifetimes are also analyzed and found to range from 2.9 to 9.1 ps. We propose that this lifetime is a good indicator of crystal quality.

## ACKNOWLEDGMENTS

The authors thank E. N. Mokhov, of The Fox Group, Inc., for the AlN used in this investigation. We also acknowledge support for this work by the National Science Foundation (ECS-0609416 and ECS-0304224) and the J. F. Maddox Foundation.

- <sup>1</sup>I. Ahmad, V. Kasisomayajula, D. Y. Song, L. Tian, J. M. Berg, and M. Holtz, *J. Appl. Phys.* **100**, 1123718 (2006).
- <sup>2</sup>V. O. Turin and A. A. Balandin, *J. Appl. Phys.* **100**, 054501 (2006).
- <sup>3</sup>A. J. Kent and J. K. Wigmore, in *Electron-Phonon Interactions in Low-Dimensional Structures*, edited by L. Challis (Oxford University Press, Oxford, 2003), Chap. 2.
- <sup>4</sup>P. G. Klemens, *Phys. Rev.* **148**, 845 (1966).
- <sup>5</sup>B. K. Ridley, *J. Phys.: Condens. Matter* **8**, L511 (1996).
- <sup>6</sup>M. Kuball, J. M. Hayes, Y. Shi, and J. H. Edgar, *Appl. Phys. Lett.* **77**, 1958 (2000).
- <sup>7</sup>D. Y. Song, M. Holtz, A. Chandolu, S. A. Nikishin, E. N. Mokhov, Y. Makarov, and H. Helava, *Appl. Phys. Lett.* **89**, 021901 (2006).
- <sup>8</sup>W. S. Li, Z. X. Shen, Z. C. Feng, and S. J. Chua, *J. Appl. Phys.* **87**, 3332 (2000).
- <sup>9</sup>D. Y. Song, S. A. Nikishin, M. Holtz, V. Soukhoveev, A. Usikov, and V. Dmitriev, *J. Appl. Phys.* **101**, 053535 (2007).
- <sup>10</sup>A. Debernardi, *Solid State Commun.* **113**, 1 (1999).
- <sup>11</sup>M. Cardona and T. Ruf, *Solid State Commun.* **117**, 201 (2001).
- <sup>12</sup>D. Y. Song, M. Basavaraj, S. Nikishin, M. Holtz, V. Soukhoveev, A. Usikov, and V. Dmitriev, *J. Appl. Phys.* **100**, 113504 (2006).
- <sup>13</sup>K. Wang and R. R. Reeber, *Thermal Expansion of GaN and AlN*, MRS Symposia Proceedings No. 482, edited by F. A. Ponce, S. P. DenBaars, B. K. Meyer, S. Nakamura, and S. Strite, (Materials Research Society, Warrendale, PA, 1998), pp. 863–868.
- <sup>14</sup>A. Link, K. Bitzer, W. Limmer, R. Sauer, C. Kirchner, V. Schwegler, M. Kamp, D. G. Ebling, and K. W. Benz, *J. Appl. Phys.* **86**, 6256 (1999).
- <sup>15</sup>A. S. Segal, S. Y. Karpov, Y. N. Makarov, E. N. Mokhov, A. D. Roenkov, M. G. Ramm, and Y. A. Vodakov, *J. Cryst. Growth* **211**, 68 (2000).
- <sup>16</sup>T. Prokofyeva, M. Seon, J. Vanbuskirk, M. Holtz, S. A. Nikishin, N. N. Faleev, H. Temkin, and S. Zollner, *Phys. Rev. B* **63**, 125313 (2001).
- <sup>17</sup>V. Yu. Davydov, Yu. E. Kitaev, I. N. Goncharuk, A. N. Smirnov, J. Graul, O. Semchinova, D. Uffmann, M. B. Smirnov, A. P. Mirgorodsky, and R. A. Evarestov, *Phys. Rev. B* **58**, 12899 (1998).
- <sup>18</sup>L. Bergman, D. Alexson, P. L. Murphy, R. J. Nemanich, M. Dutta, M. A. Strocio, C. Balkas, H. Shin, and R. F. Davis, *Phys. Rev. B* **59**, 12977 (1999).
- <sup>19</sup>K. T. Tsen, D. K. Ferry, A. Botchkarev, B. Sverdlov, A. Salvador, and H. Morkoc, *Appl. Phys. Lett.* **72**, 2132 (1998).
- <sup>20</sup>K. T. Tsen, J. G. Kiang, D. K. Ferry, H. Lu, W. J. Schaff, H. W. Lin, and S. Gwo, *Appl. Phys. Lett.* **90**, 152107 (2007).